3-D transient simulation of viscoelastic coating flows

James M. Brethour

Flow Science, Inc.
Santa Fe, New Mexico USA 87505

Presented at the 13th International Coating Science and Technology Symposium, September 10-13, 2006, Denver, Colorado[1]

Three-dimensional simulation of transient processes is typically very difficult and tedious, both for the user and the computer, as it involves creating complex meshes which must be updated during the simulation to avoid distortion during free surface movement. These difficulties are eliminated here with an Eulerian technique that tracks the fluid motion through a fixed, regular mesh. In this manner, large fluid deformations and even break-up can be computed. The computational software used for this work, ***FLOW-3D***®[1], uses **TruVOF**®, the original and true form of the Volume-of-Fluid based technique to track the free surface of the continually changing fluid domain. Added to this model is a customization to enable the simulation of viscoelastic flows.

The viscoelastic model uses a conformation tensor[2] to track the history of the deformation and rotation of each fluid element. These computations are solved alongside the conservation of mass and momentum equations already present in the flow model. Additional parameters required are the elasticity modulus and the relaxation time.

Computational results are compared to experimental results of the low-flow limit in slot coating[3] where the feed of coating liquid is gradually reduced until the downstream contact line becomes unstable. The computational results correlate well with experiments for both variations in capillary number and elasticity of the fluid.

Introduction

FLOW-3D® is a general-purpose CFD solver that is widely used in various industries to solve complex transient three-dimensional flow problems. It is especially convenient to solve free-surface problems because **TruVOF**® allows for accurate tracking of the shape and dynamics of the air-liquid interface, without needing to compute the dynamics of the gas phase. Within this solver an elastic stress solver has been implemented. The elasticity model uses a conformation tensor approach to predict the orientation, stretching and relaxation of the solution molecules. The elastic stress is extracted from this conformation tensor.

Calculation of the conformation tensor

Following on the Oldroyd-B model as proposed by Pasquali and Scriven[2], this work computes the update to the conformation tensor, **M**:

$$\frac{\partial \mathbf{M}}{\partial t} = \underbrace{-\mathbf{u}\cdot\nabla\mathbf{M}}_{\text{Change due to fluid motion}} + \underbrace{\nabla\mathbf{u}^T\cdot\mathbf{M} + \mathbf{M}\cdot\nabla\mathbf{u} + \nabla\mathbf{u} + \nabla\mathbf{u}^T}_{\text{Change due to stretching, orientation and rotation}} - \underbrace{\frac{1}{\lambda}\mathbf{M}}_{\text{Change due to relaxation}} \quad . \tag{1}$$

[1] Unpublished. ISCST shall not be responsible for statements or opinions contained in papers or printed in its publications.

Here, the equilibrium value for the conformation tensor **M** is **0**, **u** is the local fluid velocity, and λ is the relaxation time of the material. The resulting value of **M** is used to compute the elastic stress tensor:

$$\boldsymbol{\sigma} = G\mathbf{M}, \tag{2}$$

where G is the elastic modulus of the material. The total state of stress of the material is

$$\mathbf{T} = -p\mathbf{I} + \boldsymbol{\tau} + \boldsymbol{\sigma}. \tag{3}$$

where p is the fluid pressure, $\boldsymbol{\tau}$ is the viscous stress tensor and $\boldsymbol{\sigma}$ is the elastic stress tensor.

This is incorporated in the momentum transport equation for the fluid, which is

$$\frac{\partial \mathbf{u}}{\partial t} = -\mathbf{u}\cdot\nabla\mathbf{u} + \frac{1}{\rho}\left(\nabla\cdot\mathbf{T} + \mathbf{F}_\mathbf{b}\right) \tag{4}$$

which is solved along with the mass conservation constraint:

$$0 = \nabla\cdot\mathbf{u}. \tag{5}$$

Both Equations 1 and 4 are solved during each computational cycle where all of the quantities on the right side of the equation were computed during the previous computational cycle. Equation 5 is solved implicitly each cycle; the pressure and velocity component at each computational cell are adjusted iteratively until Equation 5 is satisfied to within a convergence criterion. The algorithm automatically adjusts this criterion based on the time-step size.

Low-flow limit in slot coating

The slot coating process is shown in Fig. 1. One key operability issue in slot coating is the low-flow limit; this is the minimum film thickness that can be stably applied onto a substrate for a given capillary number and the coating gap. This is important because a common goal to slot coating is applying thin films accurately. Maintaining a larger coating gap is preferred because this layout is less sensitive to variations in the coating gap.

Romero *et al.*[3] performed experiments to measure the low-flow limit observed during vacuum-assisted slot coating. Their experiments consisted of maintaining a constant web speed while gradually lowering, in steps, the liquid feed to the slot until coating bead failure occurred. The vacuum was also continuously adjusted to maintain the upstream meniscus position (see Fig. 1). The low-flow limit is reported in terms of the ratio of the coated film to the gap width.

For Newtonian flows, the low-flow limit goes down as the capillary number (Ca) is lowered. Thus, for lower web

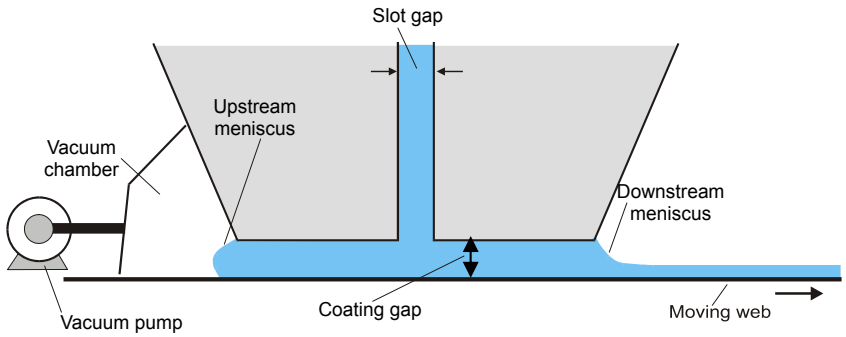

Figure 1: Two-dimensional slice of slot coating process; in the experiments, the coating gap was maintained at 100 *μm*, the slot gap was 125 *μm*, and the vacuum pressure and web speed were continously varied.

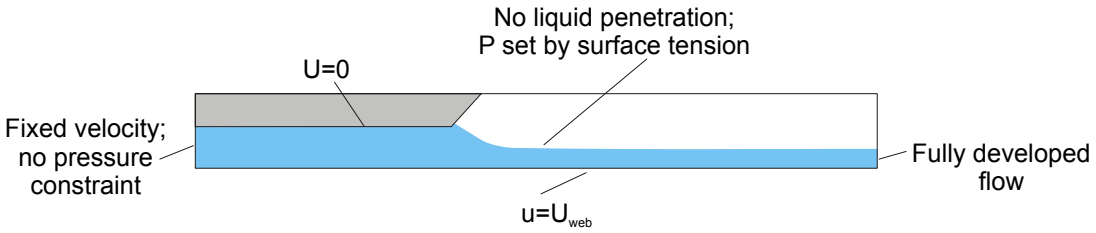

Figure 2: Computational domain and boundary conditions for the two-dimensional flow problem.

speeds, lower viscosity, or higher surface tension. Since surface tension is difficult to control, lower web speeds are antithetical to efficient operation, and lower viscosity is obtained with higher solvent loads which must be subsequently dried, a lower *Ca* is difficult to achieve. Conversely, a higher *Ca* results in higher low-flow limits. Romero *et al.*[3] noted that the presence of elasticity in the flow significantly reduced low-flow limit for the fluids used in their experiments — small concentrations of polyethylene oxide (PEO; molecular weight 4×10^6 *g/mol*) in a solution of polyethylene glycol (PEG; molecular weight 8×10^3 *g/mol*) in water. They noted that greater elasticity in the coating medium (*i.e.*, higher elastic modulus, *G*) tended to raise the low-flow limit for a given *Ca*.

In slot coating, the part of the flow critical to the maintenance of the coating bead is downstream from the slot gap. The flow rate at which the meniscus at the downstream static contact line begins to pull upstream under the die surface is the low-flow limit. Therefore, only the downstream portion of the coating bead was simulated, as the model assumes that the flow entering this part of the domain is fully developed and the imposed vacuum is sufficient to maintain the upstream meniscus. Figure 2 shows the computational domain and boundary conditions that were specified for this simulation. The computational mesh used was a fixed grid in two dimensions composed of 5872 cells (367 in the x-direction by 16 in the y-direction and each mesh cell was 12.5μm square). Table 1 shows the fluid properties of the systems considered for the simulations; a solution of 20 wt% PEG was used with three different concentrations of PEO. The simulations were performed for each fluid system by setting the web speed and then gradually lowering the inflow. The simulated low-flow limit was determined by analyzing the results for the inflow at which the downstream meniscus first begins to pull under the die. The beginning of the coating bead failure was determined by noting the point at which flow reversal began at the downstream meniscus; it is assumed that this reversal would pull the upstream meniscus under the die until air breaks through the coating bead into the vacuum chamber. This was done for a variety of web speeds.

Figure 3 is a plot of the experimental and computational results of the low-flow limits. The experiments show a greater effect of the capillary number on the low-flow limit than the computational results. However, the trends are valid and the effect of the fluid elasticity is well matched. In all cases, a rising *Ca* lowers the gap-to-thickness ratio at the low-flow limit because the shape of the downstream meniscus necessarily changes to account for the lessening

Table 1: Properties of coating fluids. All use a 20 wt.% solution of PEG in water as a base solution.

PEO (*wt%*)	Viscosity, η_0 (*mPa·s*)	Shear modulus, *G* (*Pa*)	Relaxation time, λ (*s*)
0	17.01	0.00	0.000
0.01	18.86	0.06	0.028
0.05	25.13	0.32	0.025

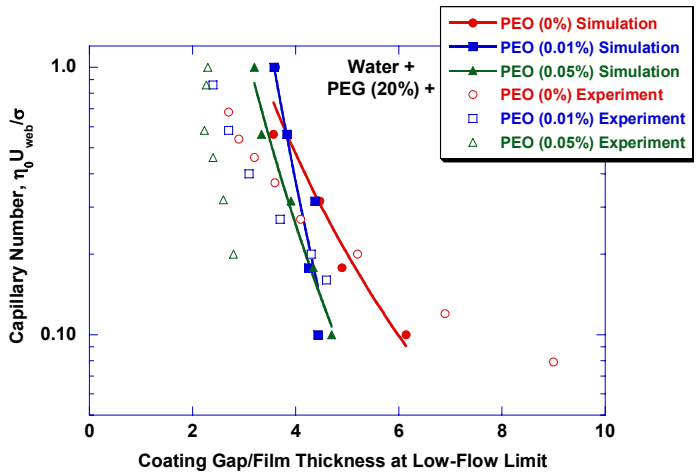

Figure 3: Plot of low flow limits in slot coating as a function of capillary number and fluid elasticity. The solid markers indicate simulation results while the open markers indicate experimental results [3]. The lines represent best-fit power-law curves.

of the surface tension effects. Also, as the elasticity of the fluid rises, the low-flow limit value shrinks. To understand this, recall that polymer coils in the solution serve to increase the resistance to extensional flow. In slot coating, the greatest extension rates occur at the downstream meniscus because the fluid surface is being stretched there and the radius of curvature is effectively lowered, which in turn lowers the gap-to-thickness ratio at the low-flow limit.

Three-dimensional slot-fed curtain coating: edge effects

Although the aforementioned work was performed as a two-dimensional simulation, the algorithm described above is also valid in three dimensions. One example is slot-fed curtain coating. Like slot coating, this is a pre-metered coating process. Its advantage is that gravity accelerates the liquid film prior to contact with the substrate, so higher coating speeds are possible before the onset of air entrainment.

Concluding remarks

The ability to simulate elastic properties of materials has been incorporated into a Volume-of-Fluid (VOF) computational fluid dynamics algorithm. Currently available is a model to simulate elastoviscoplastic materials. This work expands on this by including a conformation tensor approach and relaxation of the material, and represents work not yet available in the standard release of ***FLOW-3D***®.

---

1 ***FLOW-3D***® and **TruVOF**® are developed by and is a trademark of Flow Science, Inc., Santa Fe, New Mexico, USA.

2 M. Pasquali, L.E. Scriven. Free surface flows of polymer solutions with models based on the conformation tensor. *J. Non-Newtonian Fluid. Mech.* **108** (2002) 363-409.

3 O.J. Romero, W.J. Suszynski, L.E. Scriven and M.S. Carvalho. Low-flow limit in slot coating of dilute solutions of high molecular weight polymer. *J. Non-Newtonian Fluid. Mech*. **118** (2004) 137-156.